



Evans hole in internal modes IR spectrum of $\text{WO}_3\text{F}_3^{3-}$ ions in $(\text{NH}_4)_3\text{WO}_3\text{F}_3$ crystal

Ju.V. Gerasimova*, A.N. Vtyurin

L.V. Kirensky Institute of Physics, Russian Academy of Sciences, Siberian Branch, 660036 Krasnoyarsk, Russia

ARTICLE INFO

Article history:

Received 19 May 2011

In final form 14 December 2011

Available online 23 December 2011

ABSTRACT

Infrared absorption of $(\text{NH}_4)_3\text{WO}_3\text{F}_3$ compound has been studied. Profile of asymmetric band in 600–1000 cm^{-1} range associated with polar W–O vibrations of $\text{WO}_3\text{F}_3^{3-}$ ions is explicable on the basis of multi-oscillatory dynamics with account of damping. Complex profile with Evans holes proves that internal modes of $\text{WO}_3\text{F}_3^{3-}$ anions in the fluorine–oxygen octahedron interact due to the effects of the local field.

© 2011 Elsevier B.V. All rights reserved.

1. Introduction

Previous studies on IR absorption spectra [1,2] in ionic $\text{A}_3\text{MO}_3\text{F}_3$, in particular $(\text{NH}_4)_3\text{WO}_3\text{F}_3$, found an asymmetric profile identified as Evans hole to form by Fermi-resonance. The profile surprisingly emerged in the range of stretching W–O vibrations of $\text{WO}_3\text{F}_3^{3-}$ ions; in literature Evans holes are generally associated with hydrogen bonds [3,4]. Evans showed that occurrence of a sharp non-degenerate peak of low intensity, e.g. overtone is within an energy range of a much broader and more intensive peak of the same symmetry results in Fermi-resonance; this spectral phenomenon is schematically shown in Figure 1 [5].

It should be noted, the traditional Fermi-resonance occurs under certain conditions imposed on interacting vibrations: they should ‘mix’ in one molecule independent of the environment. Under alternative mechanism of Evans holes’ formation the vibrations may interact independent of their symmetry but through the local field of the environment. The profile formation mechanism can be formulated as follows. The field on a single molecule consists of the external field and fields of the same frequency reinduced by neighboring molecules. These neighbors have their own resonances, so the resulting field includes a frequency-dependent contribution determined by frequency offsets of the external field from these molecular vibrations.

In the high-temperature phase the symmetry of ammonium tungsten oxyfluoride $(\text{NH}_4)_3\text{WO}_3\text{F}_3$ is cubic with space group $Fm\bar{3}m$, $Z = 4$; the phase transition occurs at $T = 200$ K, the structure of the cubic phase is shown in Figure 2a, possible conformations of the octahedral ion are shown in Figure 2b [6]. There are two kinds of ammonium ions, namely, orientationally disordered ions with octahedral local symmetry and those with tetrahedral local symmetry. $\text{A}_3\text{MO}_3\text{F}_3$ crystals exhibit a special property – considerable

dipole moment in pseudo-octahedral MO_3F_3 groups orientationally disordered in the cubic phase [1]. The structure of the low-temperature phase still is not reported.

Figure 3 shows experimental IR spectrum of $(\text{NH}_4)_3\text{WO}_3\text{F}_3$ at room temperature. The range of 750–1000 cm^{-1} contains lines corresponding to stretching W–O modes of $\text{WO}_3\text{F}_3^{3-}$ ions.

Spectral range 750–1000 cm^{-1} shown in Figure 3 is similar to that in Figure 1b; the internal vibrations associated with dipole moment vibrations have not been observed to mix, which is an interesting feature of lattice dynamics of these crystals. The aim of the present study is to verify the applicability of local field effect model to the description of the observed complex spectrum profile and to determine the parameters of individual lines inside this spectrum profile.

2. Experimental

IR spectra were studied with KBr tablets containing 1% of $(\text{NH}_4)_3\text{WO}_3\text{F}_3$ crystalline powder by Vertex 70 (Bruker) spectrometer in 370–7500 cm^{-1} range with resolution 1 cm^{-1} . Temperature studies employed Specac cryostat, providing spectra in temperature range 83–523 K at stabilization accuracy ± 0.1 K.

3. Results

According to quantum-chemical calculations the trigonal C_{3v} point group (*fac*-configuration) is most probable for the fluorine–oxygen octahedra and this is proved by studies of vibrational spectra of $(\text{NH}_4)_3\text{WO}_3\text{F}_3$ [1,2]. A_1 and E vibrations in molecules of this point group are IR active. In this case stretching mode $A_1(\nu_1 = 913 \text{ cm}^{-1})$ is longitudinal, $\nu_6 = 816 \text{ cm}^{-1}$ is transversal mode [7]. From the interference-like profile in Figure 3 the suggestion may appear that vibrations ν_1 and ν_6 mix actively. Therefore it is of interest to validate if the spectrum in this range corresponds to Evans holes profile and to obtain quantitative data on parameters of spectral lines.

* Corresponding author. Fax: +7 391 2438923.

E-mail addresses: jul@iph.krasn.ru (Ju.V. Gerasimova), vtyurin@iph.krasn.ru (A.N. Vtyurin).

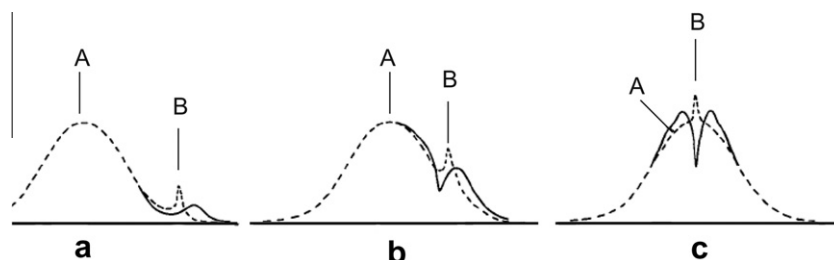


Figure 1. Spectral phenomena resulting from Fermi resonance between an intense and broad vibrational transition A and a weak and relatively sharp vibrational transition B. Cases a, b and c correspond to decreasing distances between the peak centers. Dashed line-no resonance; solid line-with resonance.

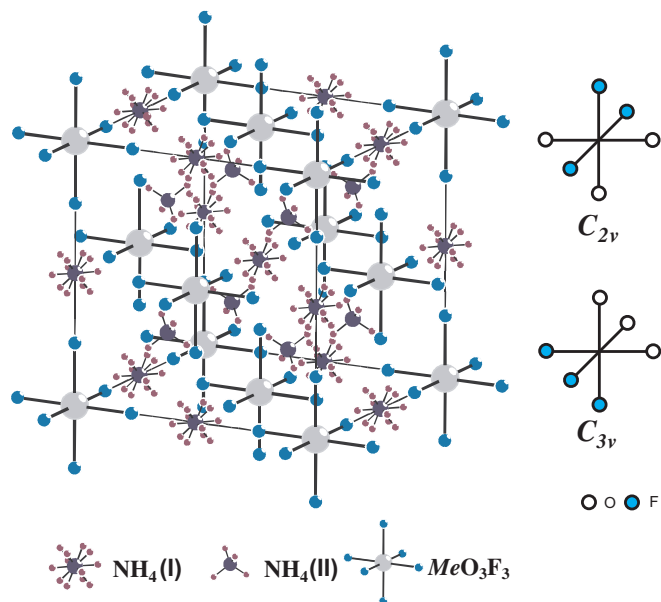


Figure 2. Structure of cubic unit cell of $(\text{NH}_4)_3\text{WO}_3\text{F}_3$ crystal at room temperature. Two possible cases of local symmetry of pseudo-octahedral $\text{WO}_3\text{F}_3^{3-}$ ion are shown to the right.

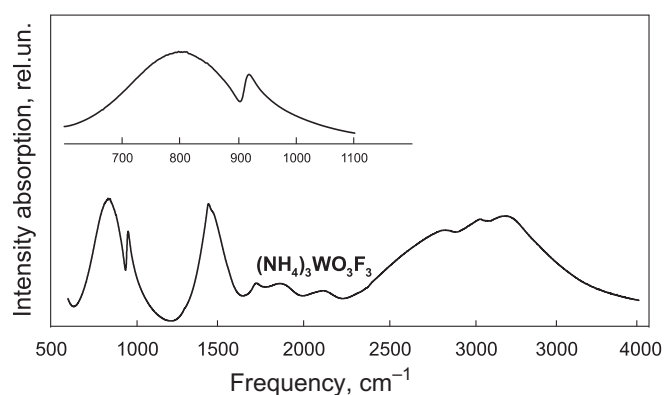


Figure 3. Experimental IR spectrum of $(\text{NH}_4)_3\text{WO}_3\text{F}_3$ at room temperature, in the insert-magnified part of W–O modes.

Bands in IR absorption spectra of $(\text{NH}_4)_3\text{WO}_3\text{F}_3$ crystal were analyzed in the range of polar W–O stretching vibrations of $\text{WO}_3\text{F}_3^{3-}$ ions on the basis of multi-oscillatory dynamics model with account of damping [8,9]. This theory was initially applied to the liquid crystals but it contains no assumptions that may preclude its application to the crystals of other kind. For the mixing mechanism we take interaction of oscillators through the local field made

by contributions (through dielectric permeability of medium ϵ) of all oscillators F .

The effect of mixing of excitations through the local field on spectral properties is qualitatively similar to manifestation of Fermi-resonance between frequency close molecular vibrations of the same symmetry but different in quantum transition order by one [8,10]. Degree of mixing by local field is substantially determined by the structure of the medium. Changes of molecular excitations mixing with thermodynamic parameters of these media should be most clearly seen around structural phase transitions. To interpret the experimental data two close resonances were considered (see Figure 4, spectrum shown by solid line). IR absorption profile is described by:

$$\epsilon'' = \frac{\omega [R_1 \Gamma_1 - I_1 (\Omega_1^2 - \omega^2)]}{(\Omega_1^2 - \omega^2)^2 + \omega^2 \Gamma_1^2} + \frac{\omega [R_2 \Gamma_2 - I_2 (\Omega_2^2 - \omega^2)]}{(\Omega_2^2 - \omega^2)^2 + \omega^2 \Gamma_2^2} \quad (1)$$

where ω is the infrared frequency, $\Omega_{1,2}$ are the frequencies of dipole-active vibrations ν_1, ν_6 , $\Gamma_{1,2}$ are the damping constants, $I_{1,2}$,

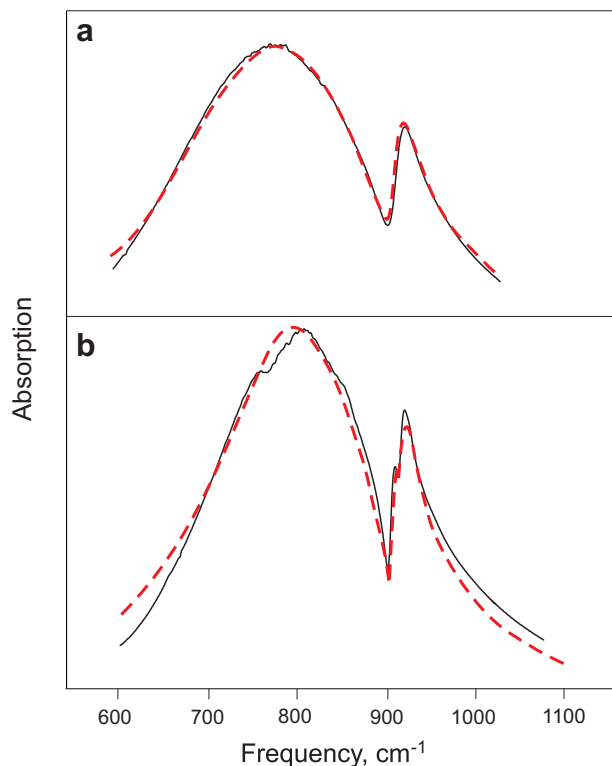


Figure 4. Profile of vibration band of $\text{WO}_3\text{F}_3^{3-}$ anions. Solid line-experiment, dash line-calculation. Details of calculation and parameter values see in the text. (a) At $T = 300$ K and (b) at $T = 92$ K.

$R_{1,2}$ are the local field factors introduced in [8,9] and taking into account effect of the molecular group on itself through the environment:

$$R_1 = \frac{[\Phi_1(1 - pq\frac{\Gamma_1}{\Omega_1}) + p^2q[\frac{1}{2}F_1 - \frac{1}{2}F_2 + \frac{q}{2}(F_1 + F_2)]]}{1 + (pq)^2 - pq\frac{\Gamma_1}{\Omega_1}} \quad (2)$$

$$I_1 = \frac{1}{2}p \frac{[F_1 - F_2 - q(\Phi_1 - \Phi_2)]}{[\Omega_1(1 + (pq)^2 - pq\frac{\Gamma_1}{\Omega_1})]} \quad (3)$$

$$\Phi_1 = \frac{1}{2}(\sqrt{F_1} + \sqrt{F_2})^2, \quad \Phi_2 = \frac{1}{2}(\sqrt{F_1} - \sqrt{F_2})^2$$

$$p = \frac{\Gamma_2 - \Gamma_1}{2(\Omega_2 - \Omega_1)} \quad (4)$$

$F_{1,2}$ are the oscillator strengths without interaction, $\Phi_{1,2}$ —with interaction. Expressions for $\Phi_{1,2}$ are taken in the limiting case of strong local field approximation. The dimensionless factor q [8,9] reflects the strength of local field effect:

$$q = \frac{\omega_2^2 - \omega_1^2}{\Omega_2^2 - \Omega_1^2}, \quad \Omega_k^2 = \frac{1}{2}(\omega_2^2 + \omega_1^2 + (-1)^k \sqrt{(\omega_2^2 - \omega_1^2)^2 + 4a^2F_1F_2}) \quad (5)$$

Here $\omega_{1,2}$ are unperturbed frequencies of the transitions that for our crystal hardly can be extracted from any spectral measurement, since they can be observed only in the hypothetical sample with diluted oxyfluoride octahedra that have their ammonium environment unperturbed, but at the same time being greatly separated from other identical octahedra. a parameter in Eq. (5) is in fact a material one that contains the density of optical electrons and anisotropy of local field. As can be seen from Eq. (5), q parameter varies from 1 if local field coincides with external field and approaches to 0 as the local field effect becomes stronger. In the present study we set this parameter as one of the parameters to be determined in the course of least square fitting procedure and have found that the best fit is obtained for $q = 0.08$. This is quite reasonable value for the case of strong local field effect, and it makes simplification of expressions for $\Phi_{1,2}$ self consistent. Other parameters to be determined in the least square fit procedure are positions and widths of resonances and oscillator strengths. Figure 4a shows overlapping profiles: the dash line—produced in formulae (1)–(3), solid line—experimental. Agreement is quite convincing. Thus, the asymmetrical profile observed in the range of polar W–O stretching modes of $WO_3F_3^{3-}$ ions is explained on the basis of multi-oscillatory model of local field.

Temperature decrease in this compound brings forth phase transition ($T = 200$ K). We should note that the spectral band of the non-degenerate vibration W–O ($\nu_1 = 913$ cm^{-1}) considerably varies with temperature; below this transition it splits into doublet. To describe the splitted profile, Eq. (1) should be modified and represented it in the following form:

$$\epsilon'' = \frac{\omega[R_1\Gamma_1 - I_1(\Omega_1^2 - \omega^2)]}{(\Omega_1^2 - \omega^2)^2 + \omega^2\Gamma_1^2} + \frac{\omega[R_2\Gamma_{21} - I_2(\Omega_{21}^2 - \omega^2)]}{(\Omega_{21}^2 - \omega^2)^2 + \omega^2\Gamma_{21}^2} + Y \frac{\omega[R_2\Gamma_{22} - I_2(\Omega_{22}^2 - \omega^2)]}{(\Omega_{22}^2 - \omega^2)^2 + \omega^2\Gamma_{22}^2} \quad (6)$$

The approximation in expression (6) neglects the difference between the effect of splitting components on each other. We introduced coefficient Y which accounts for the difference between the amplitudes of splitting components which is evident from the Raman scattering spectra of the compound under study [1,2]. This coefficient also was varied in the course of fitting procedure. The values of $F_{1,2}$, Γ_1 and Y are found to be of smaller importance for

fitting procedure than $\Gamma_{21,22}$ and $\Omega_{21,22}$. Y value is found to lie in the range 0.55–0.6 and shows no definite temperature evolution. F_1/F_2 ratio is typically equal to 1.24 while values of Ω_1 and Γ_1 are

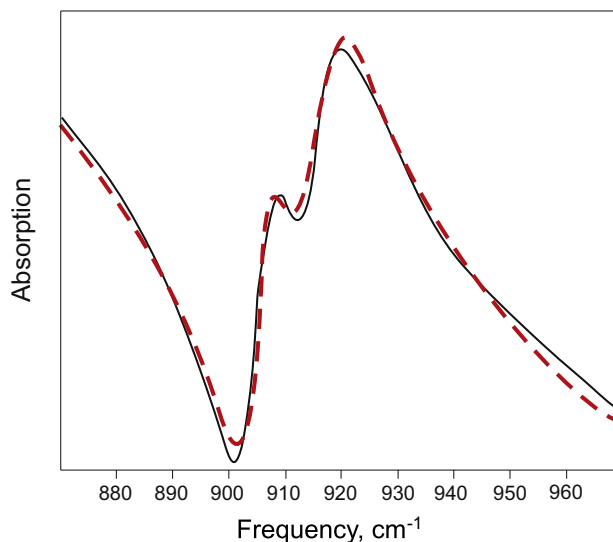


Figure 5. Doublet of W–O line ($\nu_1 = 913$ cm^{-1}) of $WO_3F_3^{3-}$ anions. Solid line—experimental spectrum, dash line—calculation ($T = 92$ K).

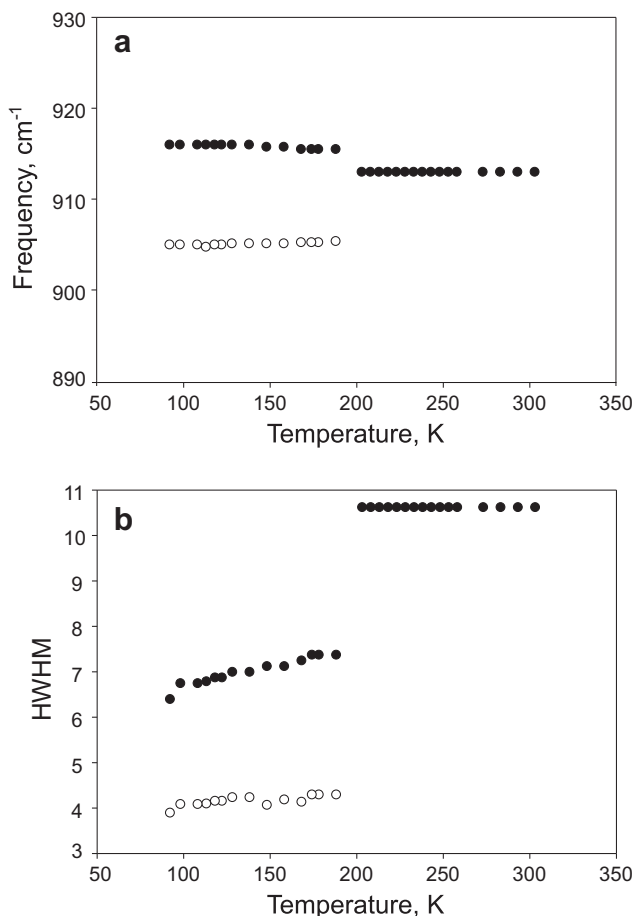


Figure 6. Temperature dependencies of (a) frequencies Ω_2 (at higher temperatures), Ω_{21} and Ω_{22} (at lower temperatures) and (b) Γ_2 (at higher temperatures), Γ_{21} and Γ_{22} (at lower temperatures) (HWHM – half widths at half-maximum) for W–O lines.

about 822 and 274–278 cm^{-1} , the evolution of them being mainly due to splitting of A_1 mode that was not included in our analysis, as discussed below.

Simulation by formula (5) is illustrated in Figure 4b. The solid line shows experimental spectrum at $T = 92$ K, the dash line—the calculated one. Figure 5 shows in more detail the splitting range of vibration A_1 . Analogous results were produced for all temperatures in 90–150 K range. It is apparent that the agreement between the experimental spectra below the phase transition temperature and the calculations is fairly good. A small discrepancy of systematic nature is that the low-frequency component of split fully symmetrical vibration is permanently shifted relative to the experimental curve towards the low frequencies. In addition, the calculated depth of Evans hole is invariable less than the experimental one. We assume these small differences to be associated with the above mentioned approximation that we used. Besides, the discrepancies can be caused by splitting of double-degenerate vibration E . Apparent in experimental spectra they could not be taken into account by our model due to small value of splitting and ambiguity of profile deconvolution. However, we believe that this simplification produces no considerable error in the analysis of the spectrum in the region of 900–950 cm^{-1} since splitting of E mode is smaller than its width.

Experimental curves analyzed by multi-oscillatory model of local field allow to investigate in more detail the vibrational dynamics in the crystal under study, Figure 6. W–O vibration at $\nu_6 = 816$ cm^{-1} is double-degenerate, however, transformation of single and fully symmetrical band $\nu_1 = 913$ cm^{-1} into doublet with decrease of temperature may evidence increasing volume of unit cell of the crystal. This is in good agreement with X-ray structural studies and analysis of Raman scattering spectra [2,11]. It is apparent that below the phase transition the width of doublet components is twice more narrow than the width of the initial line before splitting. This effect must be associated with the ordering of fluorine–oxygen octahedra. Further narrowing of the widths below phase transition temperature is much more pronounced than in cubic phase above phase transition. It can be ascribed to the gradual ordering in octahedra environment or to decrease of phonon–phonon contribution to the linewidths. More definite conclusions can be deduced when detailed study of low-temperature

phase will be available. The temperature shift of splitted modes below transition temperature becomes more noticeable, evidencing that combined influence of anharmonicity and thermal expansion coefficient in the low-temperature phase is more prominent.

4. Conclusion

Evans holes were first found in IR absorption spectra of ionic crystal. The mechanism of this phenomenon has been shown to be due to local field effect rather than Fermi-resonance. The model to describe the spectral profile in the Evans hole vicinity is applicable both for the unsplit and split narrow peak and is in good agreement with experimental results. This method substantially improves quality of analysis of spectroscopic data for a broad class of crystals.

Acknowledgments

We would like to thank Prof. E.M. Aver'yanov for discussion, and V.A. Ouskin for the technical assistance. This work has been supported by the Russian Foundation for Basic Researches, Grant No. 11-02-98002-r_sibir_a.

References

- [1] A.N. Vtyurin, Ju.V. Gerasimova, A.S. Krylov, A.A. Ivanenko, N.P. Shestakov, N.M. Laptash, E.I. Voyt, J. Raman Spectrosc. 41 (2010) 1494.
- [2] A.S. Krylov, Yu.V. Gerasimova, A.N. Vtyurin, V.D. Fokina, N.M. Laptash, Phys. Solid Stat. 48 (2006) 1356.
- [3] J.C. Evans, N. Wright, Spectrochim. Acta 16 (1960) 352.
- [4] G.D. Tewari, D.P. Khandelwal, H.D. Bist, V.P. Tayal, Can. J. Chem. 61 (1983) 2745.
- [5] J.C. Evans, Spectrochim. Acta 16 (1960) 994.
- [6] I.N. Flerov, M.V. Gorev, V.D. Fokina, A.F. Bovina, N.M. Laptash, Phys. Solid State 46 (2004) 915.
- [7] E.I. Voit, A.V. Voit, A.A. Mashkovskii, N.M. Laptash, V.Ya. Kavun, J. Struct. Chem. 47 (2006) 642.
- [8] E.M. Aver'yanov, Effects of Local Field in Liquid Crystals Optics, Science, Siberian Publishing Firm RAS, Novosibirsk, 1999.
- [9] E.M. Aver'yanov, JETP 81 (1995) 139.
- [10] M.P. Lisitsa, A.M. Yaremko, Fermi Resonance, Naukova dumka, Kiev, 1984.
- [11] I.N. Flerov et al., Phys. Solid State 50 (2008) 515.